Structure and vibrational spectra of low-energy silicon clusters

A. Sieck, D. Porezag, and Th. Frauenheim
Institut für Physik, Technische-Universität-Chemnitz, D-09107 Chemnitz, Germany

M. R. Pederson
Complex Systems Theory Branch, Naval Research Laboratory, Washington, DC 20375-5345

K. Jackson
Department of Physics, Central Michigan University, Mt. Pleasant, Michigan 48859
(Received 27 May 1997)

We have identified low-energy structures of silicon clusters with 9 to 14 atoms using a nonorthogonal tight-binding method (TB) based on density-functional theory (DF). We have further investigated the resulting structures with an accurate all-electron first-principles technique. The results for cohesive energies, cluster geometries, and highest occupied to lowest unoccupied molecular orbital (HOMO-LUMO) gaps show an overall good agreement between DF-TB and self-consistent-field (SCF) DF theory. For Si_9 and Si_{14}, we have found equilibrium structures, whereas for Si_{11}, Si_{12}, and Si_{13}, we present clusters with energies close to that of the corresponding ground-state structure recently proposed in the literature. The bonding scheme of clusters in this size range is different from the bulk tetrahedral symmetry. The most stable structures, characterized by low energies and large HOMO-LUMO gaps, have similar common subunits. To aid in their experimental identification, we have computed the full vibrational spectra of the structures, along with the Raman activities, IR intensities, and static polarizabilities, using SCF-DF theory within the local-density approximation (LDA). This method has already been successfully applied to the determination of Raman and IR spectra of silicon clusters with 3–8, 10, 13, 20, and 21 atoms. [S1050-2947(97)05512-1]

PACS number(s): 36.40.Mr, 36.40.Cg, 31.15.Ew, 31.15.Qg

I. INTRODUCTION

There is, at present, a great deal of interest in the structure and physical properties of silicon clusters, due to their potential importance in nanostructure technology. Si_n clusters have been studied by various theoretical and experimental approaches. For small n, ground-state structures have been theoretically identified using *ab initio* methods based either on Hartree-Fock (HF) theory [1,2] or density-functional (DF) theory [3–6]. Special larger clusters have also been investigated with first-principles techniques [7–9]. However, due to the increasing complexity of the energy surface on moving to larger clusters, empirical tight-binding models [10–14], which fit the neccessary matrix elements to experimental or theoretical data, and *ab initio* based tight-binding TB models [15,16], which calculate the matrix elements by quantum-mechanical methods, have been used to determine ground-state geometries and to perform molecular-dynamics for structures of various scale. Theoretical approaches which try to derive the forces neccessary for molecular dynamics (MD) from classical potentials [17–19] have also been applied.

Experimentally, the investigation of clusters contrasts to that of crystals or surfaces. For the latter, direct atomic scale structural information is available via x-ray diffraction or scanning tunneling microscopy. In the case of clusters this is not so: a combination of theoretical calculations and indirect experimental measurements must be used to determine the cluster geometries. Experimental data are available for IR and Raman spectra [20,21], photoelectron spectra [22], polarizabilities [23], mobilities [24,25], and chemical reactivities [26,27]. Ultraviolet photoelectron spectra have been calculated and compared to experiment by Chelikowsky *et al.* [28]. The reactivity of selected silicon clusters have been theoreticaly investigated by Krack and Jug [29]. For small silicon clusters the calculation of IR and Raman spectra and their experimental verification have led to the unique identification of the equilibrium structures of silicon clusters with three to seven atoms [20,21]. DF-theory-based calculations of IR and Raman spectra have already been presented for Si_3 to Si_8, Si_{10}, Si_{13} [3], Si_{20}, and Si_{21} [7]. To complete these calculations we have searched for low-energy silicon clusters with 9 to 14 atoms using our *ab initio* based nonorthogonal tight-binding (TB) method [30]. We have improved the accuracy of the method as applied to silicon and have confirmed the energetic order for the lowest energy structures with the accurate all-electron, Gaussian-orbital, density-functional (DF) code developed by Pederson *et al.* [31]. We have determined ground-state structures for Si_9 and Si_{14} and configurations for Si_{11}, Si_{12}, and Si_{13} which are energetically close to the lowest-energy structures recently presented in the literature [32–34]. For the proposed equilibrium structures of Si_9, Si_{11}, Si_{12}, and Si_{14} and for the second stable structure of Si_{13}, we have calculated the IR and Raman spectra within the local-density approximation (LDA). We hope that experimentally determined IR or Raman spectra for these cluster sizes will become available in the near future to allow for a comparison with our theoretical results.

The paper is organized as follows. In Sec. II we briefly describe the adjustment of our nonorthogonal DF-TB method

to silicon systems. In Sec. III we compare the geometries and cohesive energies of the low-energy clusters between DF-TB and SCF-LDA. Section IV contains the self-consistent calculated IR and Raman spectra and the static polarizabilities for the proposed ground-state structures of Si_9, Si_{11}, Si_{12}, and Si_{14} and for a low-energy configuration of Si_{13}. We summarize our results in Sec. V.

II. *ab initio* BASED NONORTHOGONAL TIGHT-BINDING METHOD

We have investigated the Born-Oppenheimer potential surface of silicon clusters with our nonorthogonal DF-TB method, which is described in [30,35]. This method has been successfully applied to carbon [30] and silicon [15] systems, guaranteeing a high transferability in the prediction of ground-state geometries and physical properties of various scale structures ranging from clusters, to surfaces and bulk. However, the frequencies of the high-energy vibrational modes of Si clusters described in the paper cited above [15] were found to be too large. We have removed this difficiency by determining the repulsive two-body potential by using only one structure for all distances, instead of using a combination of the Si-dimer and the diamond bulk structure. The cluster of choice consists of one central atom surrounded by four atoms in the corners of a tetrahedron. Although this structure is not the ground-state of Si_5, it represents a local stable energy minimum. For comparison, we have also used a Si_4 cluster, four atoms in the corners of a tetrahedron, to determine the repulsive potential and find a similar short-range behavior. Both repulsive potentials have the same cutoff radius $r_c = 5.2a_B$ and yield nearly identical geometries and energies for small silicon clusters. This fact confirms the transferability of the repulsive potential. The new repulsive potential results in more accurate vibrational frequencies in comparison to our previous work [15]. For example, we obtain for the three vibrational modes of the isosceles triangle Si_3 with C_{2v} symmetry within our TB approach the frequencies $128(a_1)$, $503(b_2)$, and $555(a_1)$ cm^{-1} compared to $173(a_1)$, $536(b_2)$, and $546(a_1)$ cm^{-1} in SCF-LDA. For all clusters up to Si_{14} the vibrational frequencies now range from 27 to 560 cm^{-1} in agreement with other self-consistent calculations, whereas the highest frequency modes have been strongly overestimated in the previous approach. The cohesive energies as a function of cluster size are also in an overall good agreement with scf calculations, as will be shown in the next section.

We have used the self-consistent-field (SCF)-LDA code of Pederson *et al.* [31] to confirm the energetic order of different isomers and to calculate accurate IR and Raman spectra. The DF-LDA approach is proven to yield very accurate geometries and vibrational frequencies. Despite the well known effect of overbinding, the relative total energies between different structures agree with other sophisticated *ab initio* methods. For example, Grossman and Mitas have used the computationally demanding diffusion quantum Monte Carlo calculations to determine that the icosahedral Si_{13} cluster is 0.29 eV/atom less stable than the capped trigonal antiprism with C_{3v} symmetry. Within the SCF-LDA framework they calculated nearly the same energy difference, 0.30 eV/atom [36]. Ramakrishna *et al.* [32] have compared cohesive energies, calculated with the Car-Parrinello DF method, for small silicon clusters to cohesive energies, calculated by Raghavachari *et al.* with the HF-MP4(SDQ) algorithm. They report a maximum deviation of approximately 0.1 eV/atom between the two first-principles approaches. The DF-LDA based energies were shifted to compensate for the error of the approximated exchange-correlation energy and the HF based energies were scaled to fit the experimental results. Of course the shift and scaling parameters were the same for all cluster sizes.

TABLE I. Binding energies with respect to spin polarized atoms in eV/atom and HOMO/LUMO gap in eV for silicon clusters as calculated within DF-TB and SCF-LDA.

Cluster	(sym)	E_{TB}	E_{SCF}	Gap_{TB}	Gap_{SCF}
Si2	$(D_{\infty h})$	−1.936	−1.780	0.000	0.000
Si3	(C_{2v})	−2.983	−2.965	1.874	1.008
Si4	(D_{2h})	−3.488	−3.541	1.453	1.075
Si5	(D_{3h})	−3.766	−3.825	1.702	1.976
Si6	(C_{2v})	−3.925	−4.041	1.337	2.106
Si7	(D_{5h})	−4.063	−4.187	1.511	2.097
Si8a	(C_{2h})	−4.071	−4.122	1.155	1.419
Si8b	(C_{2v})	−4.087	−4.072	0.843	1.086
Si9a	(C_{2v})	−4.176	−4.234	1.904	1.988
Si9b	(C_{2v})	−4.126	−4.183	1.846	1.551
Si9c	(D_{3h})	−4.031	−4.097	0.173	0.397
Si10a	(C_{3v})	−4.242	−4.357	1.706	2.125
Si10b	(T_d)	−4.129	−4.286	3.405	2.136
Si11a	(C_s)	−4.203	−4.274	1.214	1.041
Si11b	(E)	−4.210	−4.262	1.009	0.922
Si11c	(C_s)	−4.205	−4.259	1.330	1.073
Si12a	(C_s)	−4.228	−4.274	0.925	0.593
Si12b	(E)	−4.250	−4.267	0.862	0.940
Si13a	(C_{3v})	−4.204	−4.305	1.451	1.606
Si13b	(C_{2v})	−4.277	−4.291	1.332	0.787
Si14a	(C_s)	−4.328	−4.372	1.531	1.774
Si14b	(C_s)	−4.300	−4.332	1.029	1.323
Si14c	(D_{3h})	−4.283	−4.253	1.095	0.896
Si14d	(C_{3v})	−4.179		0.000	

III. GEOMETRIES AND ENERGIES, A COMPARISON BETWEEN DF-TB AND SELF-CONSISTENT DF-LDA

For small silicon clusters up to Si_8, we determine within the DF-TB method the same equilibrium structures as Fournier *et al.* [4] and Pederson et al. [3]. These are for Si_3 the isosceles triangle with C_{2v} symmetry, for Si_4 the rhombus (D_{2h}), for Si_5 the compressed trigonal bipyramid (D_{3h}), for Si_6 the edge capped trigonal bipyramid (C_{2v}), for Si_7 the compressed pentagonal bipyramid (D_{5h}), and for Si_8 the distorted bicapped octahedron (C_{2h}). Overall, there is good agreement between the SCF-LDA and DF-TB methodologies for geometrical parameters and binding energies for these small clusters. The deviations in bond lengths and angles are smaller than 10%. The deviations in cohesive energies are smaller than 4% for all clusters larger than Si_2, see Table I.

Considering larger clusters with 9 to 14 atoms, we have

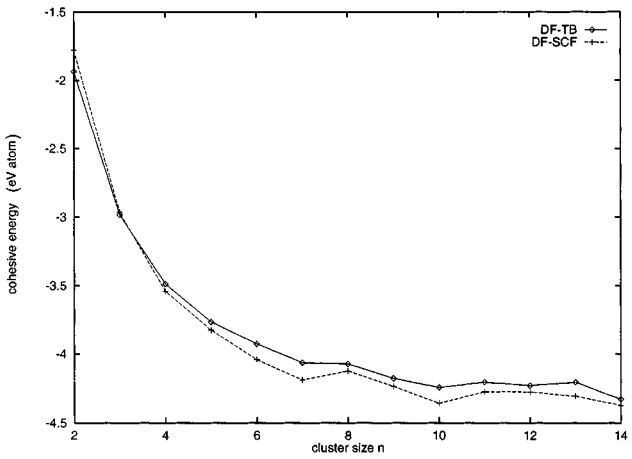

FIG. 1. Cohesive energies in eV/atom as a function of cluster size as calculated within DF-TB and SCF-LDA.

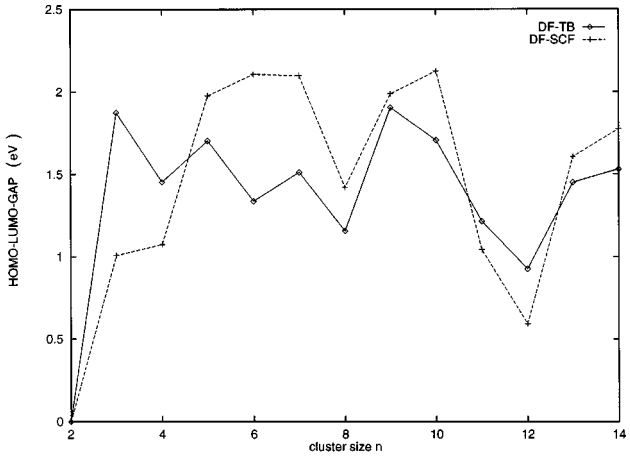

FIG. 2. HOMO/LUMO gap in eV as a function of cluster size as calculated within DF-TB and SCF-LDA.

started our search for the equilibrium structures with different seed clusters obtained by edge or face capping of smaller stable clusters or with clusters taken from the literature. We have optimized these structures with our DF-TB method by applying either a stochastic molecular-dynamic quenching or conjugate gradient relaxation until the maximum force on every atom dropped below 10^{-4} Hartree/Bohr. At least the two most stable DF-TB structures (most stable in the sense of lowest energy and not lowest reactivity) were then relaxed with the SCF-LDA code using a $6s5p3d$ basis set (i.e., 6 s-like, 5 p-like, and 3 d-like contracted Gaussians). The minimum allowed force during these conjugate gradient procedure has been 10^{-3} Hartree/Bohr.

Within SCF-LDA we calculate the cohesive energies with respect to spin polarized isolated atoms. Since the DF-TB method does not take spin into account, we have shifted the DF-TB energies by the spin-polarization energy of 0.656 eV. The cohesive energies and highest occupied to lowest unoccupied molecular orbital (HOMO-LUMO) gaps for the lowest energy clusters are summarized in Table I. The variation of both quantities with cluster size is depicted in Figs. 1 and 2. Si_7, Si_{10}, and Si_{14} are more stable than their neighbors. The order of the DF-TB determined cohesive energies of the lowest-energy structures for one cluster size agrees with the SCF-LDA results for all smaller clusters and Si_9, Si_{10}, and Si_{14} but is reversed for Si_8, Si_{11}, Si_{12}, and Si_{13}. Please note that for the three latter clusters the differences in the scf cohesive energies are smaller than 0.02 eV/atom, which certainly is below the accuracy of the DF-TB approach. The variation of the HOMO-LUMO gap as calculated within DF-TB with increasing cluster size n is in good agreement with the SCF-LDA calculations for $n>7$. The quantitative differences for Si_8 to Si_{14} are at maximum of 20%, whereas the deviations increase with decreasing cluster size. Note that an accurate description of unoccupied orbitals often fails due to the use of a minimum basis set.

We now discuss the results for each cluster size considering only the self-consistent calculated cohesive energies and HOMO-LUMO gaps. Tables for the bondlengths and angles of the low-energy clusters as calculated within DF-TB and SCF-LDA are available upon request.

Si_9. We found two stacked distorted rhombi with an additional atom capped on top (Si_{9a}) to be the lowest-energy cluster [see Fig. 3(a)]. This structure has C_{2v} symmetry and is 0.05 eV/atom more stable than the distorted tricapped trigonal prism Si_{9b}, first proposed by Ordejon *et al.* [13] as the most stable structure of Si_9. Raghavachari and Rohlfing [1] calculated by using a HF-MP4(SDQ)/6-31G* algorithm nearly identical energies for a tricapped trigonal prism $Si_{9c}(D_{3h})$, a tricapped octahedron (C_{3v}), and a distorted tricapped octahedron (C_s). They found the latter cluster to be only 0.014 eV/atom more stable than the first one and only 0.011 eV/atom more stable than the second. Ordejon *et al.* found by using a non-SCF multicenter TB approach [37] an energy difference of 0.10 eV/atom between the distorted tricapped octahedron (C_s) and the distorted tricapped trigonal prism $Si_{9b}(C_{2v})$. We calculated an energy difference of 0.09 eV/atom between the triplet state of the tricapped trigonal prism (D_{3h}) [which is nearly isoenergetic to the distorted tricapped octahedron (C_s)] and Si_{9b}. This confirms the energy difference between the three structures considered by Raghavachari and Rohlfing and the structure proposed by Ordejon. However, none of these authors considered our candidate Si_{9a} (C_{2v}). It is possible that a similar structure has been described in earlier works of Ballone *et al.* [7] and of Wales [18], but due to the lack of information about geometrical parameters we cannot verify this. Note that Si_{9a} has a large gap of 2.0 eV within the SCF-LDA formalism.

Si_{11}. We confirm a structure Si_{11a} proposed by Lee *et al.* [33] using a TB method to be the most stable Si_{11} cluster. They describe the geometry as a distorted tricapped tetragonal antiprism, but it may also be seen as a distorted pentacapped trigonal prism [see Fig. 3(b)]. The three rectangular faces of the prism, one edge and one triangular face are capped, which results in C_s symmetry. The relaxation out of different starting structures for Si_{11} with the TB method has also spawned another cluster Si_{11b} having no symmetry at all. This cluster is only 0.01 eV/atom less stable than Si_{11a}. It is a distorted 4-5 prism, with two atoms capping the fivefold ring [see Fig. 3(c)]. Structure Si_{11a} is more stable by 0.02 eV/atom within the DF-TB method than the pentacapped trigonal prism with C_{2v} found by Rohlfing and

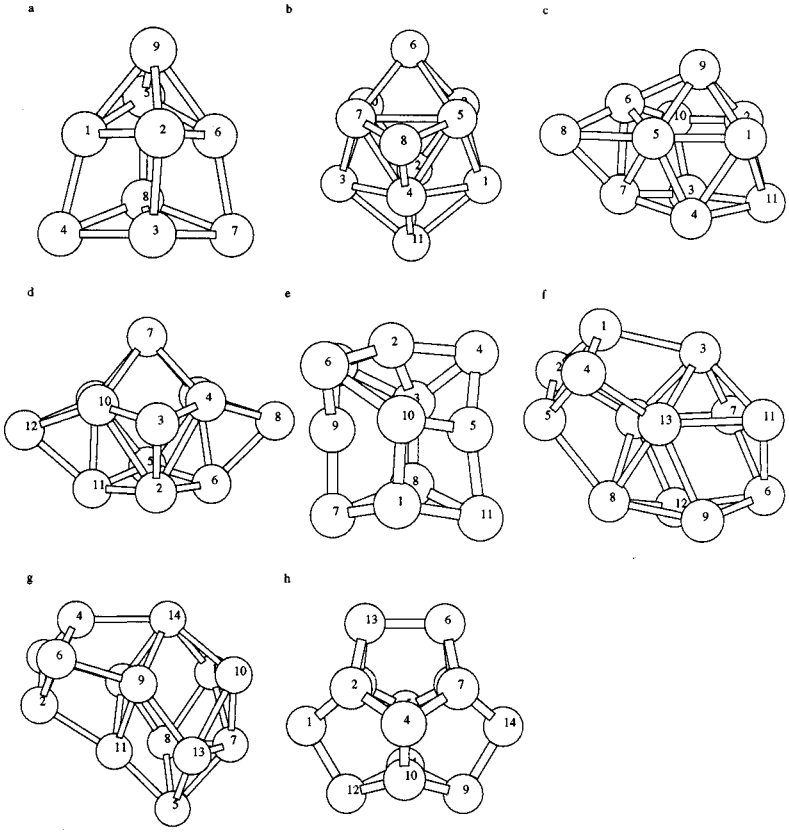

FIG. 3. Shown above are the geometries for (a) $Si9_a$, (b) Si_{11a}, (c) Si_{11b}, (d) Si_{12a}, (e) Si_{12b}, (f) Si_{13b}, (g) Si_{14a}, (h) Si_{14c}.

Raghavachari [38]. Grossman and Mitas [9] considered three stacked triangles with capped tops (D_{3h}) for Si_{11}. We calculated this cluster to be metastable with a binding-energy 0.03 eV/atom higher than the one of Si_{11a}. After small displacements in the direction of the occuring imaginary eigenmodes this structure converges within the DF-TB approach to Si_{11b}.

Si_{12}. Recently Ramakrishna *et al.* have presented results of their extensive search for the ground state of Si_{12} [32]. They report on six isomers, which differ by only 0.02 eV/atom in cohesive energies, as calculated within the DF-LDA. These isomers can all be described either as hexacapped trigonal prisms or antiprisms with different faces capped. They additionally report on seven other structures with the highest energy cluster being only 0.11 eV/atom less stable than the lowest energy one. Considering their isomer 2 (Si_{12a}), a hexacapped distorted trigonal prism with (C_s) symmetry [see Fig. 3(d)], we obtain a cohesive energy of -4.274 eV/atom. We also find another, nonsymmetric, structure Si_{12b} [see Fig. 3(e)] to be only 0.01 eV/atom less stable than their isomer 2. This structure, a stacking sequence of a distorted rhombus, a fourfold ring, a triangle and a single atom, does not match any of their isomers.

Si_{13}. The most stable structure of Si_{13} consists of four stacked triangles with a cap on top. Recent QMC [36] and DF-LDA [3,34] calculations found this structure Si_{13a} to be favored against the icosahedral form of Si_{13}. From the present search we predict the cohesive energy of another structure to be very close to that of the lowest energy cluster. This structure, Si_{13b}, has C_{2v} symmetry and can be described as a distorted tricapped trigonal prism with an additional rhombus capped on one edge of the prism [see Fig. 3(f)]. The energy difference between these two structures is

TABLE II. Vibrational frequencies of lowest-energy silicon clusters as calculated within DF-LDA.

Cluster	(Sym)	Frequencies (cm^{-1})
Si_{9a}	(C_{2v})	56(b_2),109(b_1),120(a_2),164(a_1),219(a_1), 225(b_2),256(b_1),262(b_2),284(a_1),285(a_2), 290(b_1),292(a_1),322(a_1),332(a_1),335(b_1), 373(a_2),397(b_1),405(a_1),437(b_2),468(b_2), 486(a_1)
Si_{11a}	(C_s)	62, 111, 115, 129, 149, 197, 208, 223, 232, 251, 253, 261, 268, 278, 281, 298, 304, 306, 350, 354, 358, 366, 397, 411, 413, 439, 493
Si_{12a}	(C_s)	46, 110, 139, 163, 166, 178, 196, 197, 213, 228, 234, 238, 243, 255, 264, 266, 288, 291, 313, 322, 336, 342, 345, 390, 407, 425, 471, 488, 506
Si_{13b}	(C_{2v})	45(b_2),58(b_1),100(a_2),136(b_1),145(a_1), 158(a_2),168(b_2),176(b_1),189(a_1),199(b_2), 204(a_1),229(a_2),230(a_2),230(b_1),233(a_1), 255(a_1),257(b_2),259(b_2),279(a_2),289(a_1), 302(b_2),311(b_1),330(a_1),349(b_1),351(a_1), 353(a_2),356(b_2),360(a_2),373(a_1),394(a_1), 405(b_2),408(b_1),446(b_1),454(a_1)
Si_{14a}	(C_s)	54, 99, 103, 115, 142, 154, 180, 188, 193, 196, 213, 222, 223, 230, 240, 259, 269, 273, 283, 286, 290, 298, 306, 315, 339, 356, 356, 365, 367, 370, 401, 410, 428, 447, 463, 480

only 0.014 eV/atom, whereas Grossman and Mitas found an energy difference of 0.3 eV/atom between the icosahedral cluster and Si_{13a} within the DF-LDA [36]. The HOMO-LUMO gap of our structure Si_{13b} is only half the gap of the most stable cluster Si_{13a}.

Si_{14}. Only a few structures for Si_{14} have been presented in the literature so far. We suggest a stacking sequence of two distorted rhombi, one fivefold ring, and an atom on top (Si_{14a}) as a candidate for the equilibrium structure. In this cluster the longer axes of the two stacked rhombi are perpendicular, as can be seen in Fig. 3(g). There exist also a local stable cluster Si_{14b} with similar geometry but parallel longer axes, which is only 0.04 eV/atom higher in energy. Another local stable isomer is the octacapped trigonal prism with D_{3h} symmetry (Si_{14c}). The rectangular faces of the prism are capped by a sixfold ring and both triangular faces by one atom [see Fig. 3(h)]. This geometry is 0.12 eV/atom less stable than the lowest energy candidate. One interesting feature of this structure are the six fivefold rings, which also occur in the tetrahedral bulk structure. Si_{14c} has 30 bonding angles very close to 109°. For the three structures Si_{14a}, Si_{14b}, and Si_{14c} the HOMO-LUMO gaps are 1.77, 1.32, and 0.90 eV, respectively. Within the DF-TB method the lowest-energy cluster is more stable by 0.15 eV/atom than the four stacked triangles with capped tops (Si_{14d}), investigated by Grossman *et al.* [9].

Very recently Ho and co-workers have presented candidates for the ground-state isomer of silicon clusters from Si_{11} to Si_{20} using a genetic algorithm and a tight-binding potential [39]. Similarly to our approach they further relaxed their new candidates within the LDA. Their most stable structures for Si_{12} and Si_{14} are identical to the clusters we have found, but for Si_{13} Ho *et al.* calculated our cluster Si_{13b} to be more stable than cluster Si_{13a} by 0.02 eV/atom. The small deviations in binding energies and HOMO-LUMO gaps between both LDA approaches are probably due to the usage of different basis sets and different functionals for the exchange and correlation potential.

All considered structures, with the exception of Si_{9a}, have a tricapped trigonal prism as a common subunit. This building block can also be described as a stacking sequence of a rhombus, a rectangle and a single atom capped on top. In the most stable nine atom cluster Si_{9a}, the rectangle is replaced by a rhombus. The tetracapped trigonal prism Si_{10a} (C_{3v}) can be obtained by capping one top of the tricapped trigonal prism. Further capping of one edge of the prism leads to the Si_{11a} cluster. Capping of the second triangle followed by a displacement of the edge capping atom of Si_{11a} to one side of the trigonal prism results in structure Si_{12a}. In Si_{13b} a rhombus is attached to four atoms of the tricapped trigonal prism. Si_{13a} can be obtained by adding a further triangle to the three stacked triangles and capping the top. Si_{14a} is very similar to Si_{13b}, the rectangle in the building block is expanded to a fivefold ring in Si_{14a}. Si_{14c} can be built by replacing the capping atoms of the tricapped trigonal prism with three dimers and capping each of the two triangular faces with one atom. The dimers lie in the mirror plane perpendicular to the principal axis. All considered low-energy structures with 11 to 14 atoms have various fivefold and even sixfold coordinated atoms. The overall bonding scheme is quite different from the bulk tetrahedral symmetry, but each structure has numerous bond angles close to 109°.

IV. VIBRATIONAL SIGNATURES AND POLARIZABILITIES

Due to the small differences in cohesive energies for the low-energy clusters, theoretical data for the identification of the ground-state geometry of a cluster are highly useful. Calculation of the vibrational spectra not only confirms the stable stationary points on the Born-Oppenheimer surface, but along with the Raman activities and IR absorption intensities also provides unique spectral information on chemical bonding, which can be used for comparisons with experiment. This approach has already been successfully applied to identify smaller clusters [20,21].

To determine the vibrational modes of the clusters we apply the method discused in Refs. [3,7,40,41]. For the numerical computation of the vibrational frequencies, we used displacements of $0.05a_B$ and for the computation of the dynamical response to an external electric field, we used small electric field components of $\Delta G = 0.005$ a.u. As described in [7], the SCF-DF method yields reliable results for vibrational frequencies, IR intensities, and Raman activities of small silicon clusters with a $(6s5p3d)$ basis set and within the LDA. Since the IR and Raman activities depend on second and third order total energy derivatives with respect to the normal mode coordinates and external electric field components, extremely well converged energies and electronic densities are required. Hence for the calculation of the vibrational frequencies, we have converged the total energy to 10^{-6} Hartrees and for the calculation of the intensities and activities to 10^{-8} Hartrees with respect to the electronic degrees of freedom.

We now discuss the IR and Raman spectra of our candidates for the ground-state structures of Si_9, Si_{11}, Si_{12}, and Si_{14} and for the second stable structure of Si_{13}. Table II contains the vibrational frequencies of these clusters labeled by the symbol of the irreducible representations for clusters with more than two symmetry elements.

Si_{9a}. This cluster has C_{2v} symmetry and therefore has no degenerate eigenmodes. All modes are Raman active, but only the modes which transform as the irreducible representations a_1, b_1, and b_2 are IR active. Therefore one expects a maximum number of 21 Raman active modes and a maximum number of 18 IR active modes. On the left-hand side of Fig. 4, we present the predicted IR and Raman spectra for Si_{9a}. The lower panel shows the Gaussian-broadened vibrational density of states (VDOS), obtained by centering a Gaussian function with a full width at half maximum (FWHM) of 6 cm^{-1} on each of the normal mode frequencies. In the other panels the VDOS is weighted by the IR intensity and Raman activity of the various modes. For the Raman spectra we plot the activities for parallel and perpendicular polarizations.

The IR spectrum has its strongest peak at 486 cm^{-1} and six other strong peaks are located in the range from 109 to 468 cm^{-1}. The maximum IR intensity of 0.16 $(D/Å)^2$/amu is small compared to some spectra of other structures such as Si_4 [1.34 $(D/Å)^2$/amu] or Si_{10}(TCO) [1.5 $(D/Å)^2$/amu] in Ref. [3]. In the experimental spectra of Ref. [21] only the

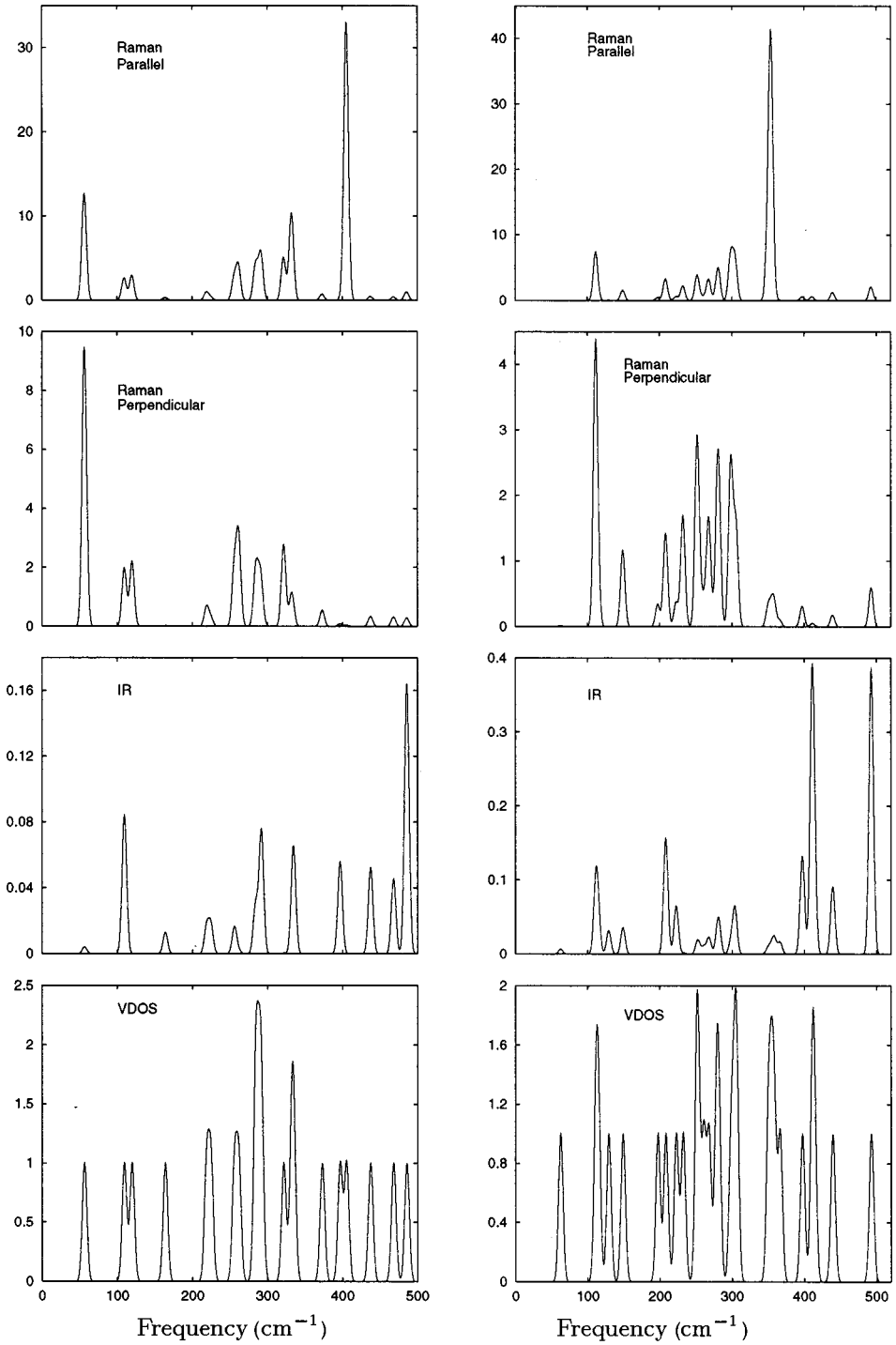

FIG. 4. VDOS and simulated IR and Raman spectra for the Si_{9a} structure (left) and for the Si_{11a} structure (right). IR intensities are in $(D/Å)^2$/amu and Raman activities are in $Å^4$/amu.

modes corresponding to IR intensities greater than approximately 0.15 $(D/Å)^2$/amu (within DF-LDA) could be identified.

Si_{9a} has a fully polarized strongest Raman peak at 405 cm^{-1} and one strong peak at 56 cm^{-1}, which is nearly nonpolarized (note the different scaling in the Raman perpendicular and Raman parallel DOS).

Si_{11a}. This structure has only one reflection plane, hence all 27 modes are nondegenerate and both Raman and IR active. As can be seen on the right hand side of Fig. 4, Si_{11a} has two nearly equally strong IR active modes at high energies (411 and 493 cm^{-1}) and only one partly polarized strong Raman peak at 354 cm^{-1}. All Raman peaks observed in the direction perpendicular to the polarization plane have very low intensities. Since the only difference between Si_{11a} and Si_{10a} (TTP) is the additional atom capped on one edge of the trigonal prism, it is interesting to see the influence of the additional atom on the IR and Raman spectra (the spectra for Si_{10a} were presented in Ref. [3]). Both structures have one highly active and strongly polarized Raman mode at about 350 cm^{-1}. The Raman-perpendicular spectra is very weak for both clusters. The IR spectra of both structures are weak, too, but the highest energy IR active modes occur at higher energies for Si_{11a}.

Si_{12a}. As with Si_{11a} this cluster has only nondegenerate vibrational modes, which are all Raman and IR active. The

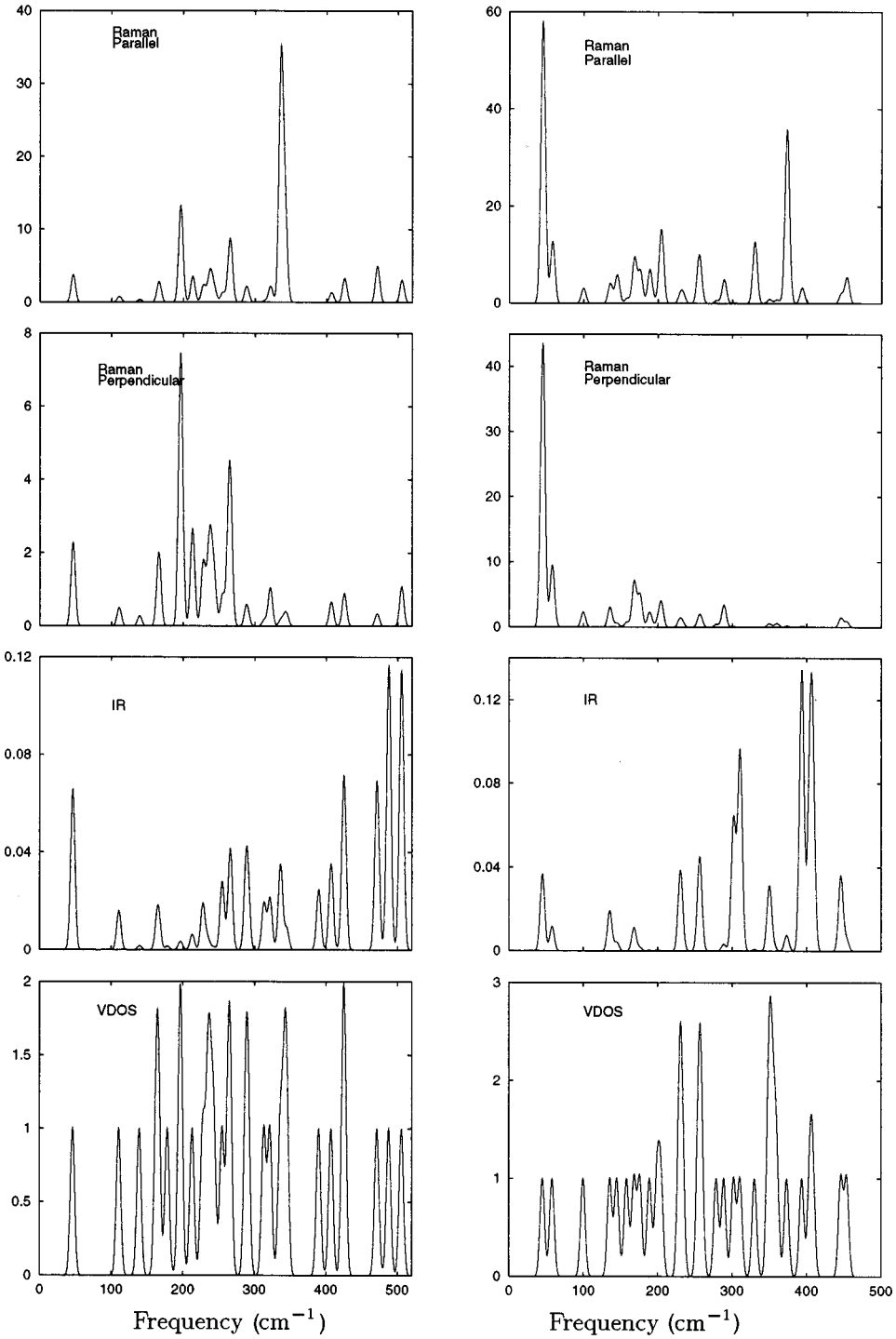

FIG. 5. VDOS and simulated IR and Raman spectra for the Si $_{12a}$ structure (left) and for the Si $_{13b}$ structure (right). IR intensities are in (D/Å)^2/amu and Raman activities are in Å^4/amu.

IR and Raman spectra of Si_{12a} are depicted on the left-hand side of Fig. 5. The former is rather weak and may be hard to detect experimentally. The strongest, polarized, Raman peak for Si_{12a} is at 336 cm^{-1}, whilst two other strong Raman peaks appear at 196 and 342 cm^{-1}, the latter obscured by the 336 cm^{-1} peak in the diagram.

Si $_{13b}$. The second most stable configuration of Si_{13} we found has C_{2v} symmetry and therefore has a maximum number of 33 Raman and 27 IR active modes. The IR absorption intensities are rather weak and may be difficult to observe in experiment. The most striking feature in the Raman spectra is a strong peak with low energy (45 cm^{-1}). Si_{13b} has another strong, polarized, peak at 373 cm^{-1} (see the right-hand side of Fig. 5).

Comparison of the spectra for Si_{13b} with the spectra of the proposed ground-state sructure Si_{13a} in Ref. [3] is helpful in the identification of the ground state. The IR spectra of both Si_{13} isomers are very weak and therefore of little use in an experimental identification. In contrast to the IR spectrum, the Raman spectra are well suited for an experimental determination of the ground-state structure of Si_{13}, because they are strikingly different. Si_{13a} has strong Raman modes at 100, 220, and 337 cm^{-1}, the strongest mode at 337 cm^{-1} being fully polarized. Considering that the Si_{13a} structure is

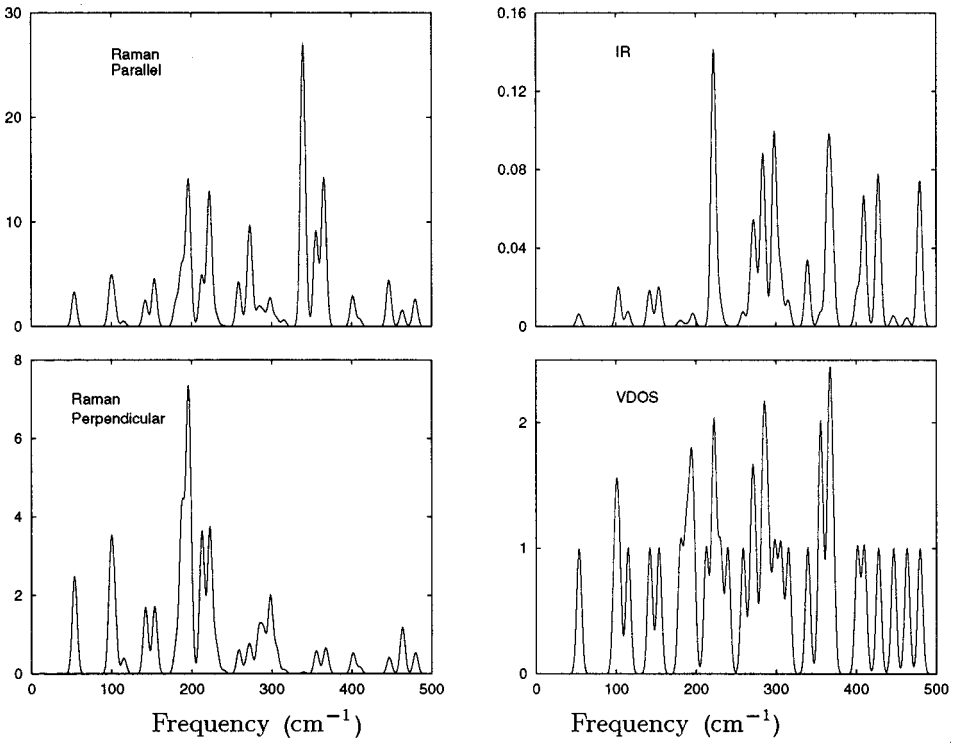

FIG. 6. VDOS and simulated IR and Raman spectra for the Si_{14a} structure. IR intensities are in $(D/Å)^2$/amu and Raman activities are in $Å^4$/amu.

only 0.01 eV/atom more stable than the Si_{13b} structure within DF-LDA, it would be very useful to determine the experimental Raman-spectra of Si_{13} clusters.

Si_{14a}. Since our ground-state candidate for Si_{14} has C_s symmetry, all of its 36 vibrational modes are both IR and Raman active. The Raman spectra, which are depicted in Fig. 6 along with the IR spectrum, show one high active mode at 339 cm^{-1}, which is strongly polarized, and five less active peaks located in the range from 196 to 365 cm^{-1}. The most active IR modes have frequencies larger than 200 cm^{-1}. The strongest has an intensity of ≈ 0.14 $(D/Å)^2$/amu, only and therefore, it is near the experimentally detectable limit. Although structure Si_{14a} is similar to Si_{13b} (the rectangle in Si_{13b} is replaced by a fivefold ring), both the IR intensities and the Raman activities are quite different.

In Table III we present the static electric dipole moments for the investigated clusters and compare the calculated static polarizabilities with the experimental measurements of Schäfer *et al.* [23]. We define the polarizability α as the averaged sum over the eigenvalues α_i of the polarizability tensor $\alpha=(\alpha_1+\alpha_2+\alpha_3)/3$. Our calculations of the polarizabilities show smaller variations with cluster size than has been observed in experiment. The measured polarizabilities range from 1.8 to 5.5 $Å^3$/atom, whereas the calculated polarizabilities are all greater than 4.34 Å/atom and less than 5.21 Å/atom. This deviation between theory and experiment has previously been mentioned in Ref. [3] for Si_{10}, Si_{13}, Si_{20}, and Si_{21}. Due to the small differences in calculated polarizabilities for Si_{13a} (4.40 $Å^3$/atom) and Si_{13b} (4.51 $Å^3$/atom) and for both Si_{10} isomers (TTP and TCO), we expect that consideration of other isomers will not resolve the discrepancy between theory and experiment.

Recently, Vasiliev *et al.* have presented *ab initio* calculations for the polarizabilities and dipole moments of Si_1 to Si_{10} [42]. Our calculations are in excellent agreement with their results for all considered silicon clusters.

V. SUMMARY

We have compared the results for geometrical parameters, binding energies, vibrational frequencies, and HOMO-LUMO gaps between DF-TB and SCF-LDA and find that the TB approach is a reasonably accurate method for searching for the lowest-energy structures of silicon clusters. We have presented ground-state candidates for Si_9 and Si_{11} to Si_{14}. Despite the large number of possible configurations, the most stable structures with 9 to 14 atoms have all a common similar subunit. The differences in energy between the two most stable structures for clusters in this size range

TABLE III. Dipole moments and polarizabilities as calculated within DF-LDA. Experimental results for clusters are taken from Ref. [23] and results for Si_1, Si_{10a}, Si_{13a}, Si_{20}, and Si_{21} are taken from Ref. [3].

Cluster	$\lvert\mu_{LDA}\rvert$(D)	α_{LDA} ($Å^3$/atom)	α_{expt} ($Å^3$/atom)
Si_1	0.00	5.88	5.4
Si_3	0.32	5.21	
Si_4		5.07	
Si_5		4.82	
Si_6	0.21	4.51	
Si_7		4.41	
Si_{8a}		4.54	
Si_{9a}	0.28	4.43	2.9
Si_{10a}	0.72	4.34	5.5
Si_{11a}	0.76	4.38	2.8
Si_{12a}	0.94	4.50	2.3
Si_{13a}	0.12	4.40	1.8
Si_{13b}	0.30	4.51	1.8
Si_{14a}	1.12	4.47	2.7
Si_{20}	0.02	4.83	3.6
Si_{21}	0.79	4.58	3.1

are ≈ 0.01 eV/atom, only. To allow for a unique spectral identification we have calculated the IR and Raman spectra for the lowest-energy configurations. Since the calculated IR absorption intensities for Si_{9a}, Si_{12a}, Si_{13b}, and Si_{14a} are rather weak, one can conclude that Raman experiments should be better suited for the identification of the ground states in these cases. In contrast to experiment, our computed static polarizabilities show smaller variations with increasing cluster size. The determination of the structure of the observed clusters and an improvement of the experimental accuracy is required to fully understand these differences.

ACKNOWLEDGMENTS

We gratefully acknowledge support from the Deutsche Forschungsgemeinschaft, the Deutscher Akademischer Austauschdienst, and National Science Foundation Grant No. INT-9514714. M.R.P. gratefully acknowledges partial support from the ONR Georgia Tech molecular design institute (Grant No. N00014-95-1116) and computational support from the Department of Defense High Performance Computing Centers. K. J. gratefully acknowledges support from National Science Foundation Grant No. RU1-DMR940985.

[1] K. Raghavachari and C. M. Rohlfing, J. Chem. Phys. **89**, 2219 (1988).
[2] C. M. Rohlfing and K. Raghavachari, J. Chem. Phys. **96**, 2114 (1992).
[3] K. Jackson, M. R. Pederson, D. Porezag, Z. Hajnal, and Th. Frauenheim, Phys. Rev. B **55**, 2549 (1997).
[4] R. Fournier, S. B. Sinnott, and A. E. DePristo, J. Chem. Phys. **97**, 4149 (1992).
[5] N. Binggeli and J. R. Chelikowsky, Phys. Rev. B **50**, 11 764 (1994).
[6] P. Ballone, W. Andreoni, R. Car, and M. Parrinello, Phys. Rev. Lett. **60**, 271 (1988).
[7] M. R. Pederson, K. Jackson, D. V. Porezag, Z. Hajnal, and Th. Frauenheim, Phys. Rev. B **54**, 2863 (1996).
[8] E. Kaxiras and K. Jackson, Phys. Rev. Lett. **71**, 727 (1993).
[9] J. C. Grossman and L. Mitas, Phys. Rev. B **52**, 16 735 (1995).
[10] L. Goodwin, A. J. Skinner, and D. G. Pettifor, Europhys. Lett. **9**, 701 (1989).
[11] I. Kwon, R. Biswas, C. Z. Wang, K. M. Ho, and C. M. Soukoulis, Phys. Rev. B **49**, 7242 (1993).
[12] M. Menon and K. R. Subbaswamy, Phys. Rev. B **51**, 17 952 (1995).
[13] P. Ordejon, D. Lebedenko, and M. Menon, Phys. Rev. B **50**, 5645 (1994).
[14] D. Tomanek and M. A. Schluter, Phys. Rev. B **36**, 1208 (1987).
[15] Th. Frauenheim, F. Weich, Th. Köhler, S. Uhlmann, D. Porezag, and G. Seifert, Phys. Rev. B **52**, 11 492 (1995).
[16] O. F. Sankey and D. J. Niklewski, Phys. Rev. B **40**, 3979 (1989); O. F. Sankey, D. J. Niklewski, D. A. Drabold, and J. D. Dow, *ibid.* **41**, 12 750 (1990).
[17] J. R. Chelikowsky, K. M. Glassford, and J. C. Phillips, Phys. Rev. B **44**, 1538 (1991).
[18] D. J. Wales and M. C. Waterworth, J. Chem. Soc. Faraday Trans. **88**, 3409 (1992).
[19] X. G. Gong, Phys. Rev. B **47**, 2329 (1993).
[20] E. C. Honea, A. Ogura, C. A. Murray, K. Raghavachari, W. O. Sprenger, M. F. Jarrold, and W. L. Brown, Nature (London) **366**, 42 (1993).
[21] S. Li, R. Z. Van Zee, W. Weltner, Jr., and K. Raghavachari, Chem. Phys. Lett. **243**, 275 (1995).
[22] O. Cheshnovsky, S. H. Yang, C. L. Pettiette, M. J. Craycraft, Y. Liu, and R. E. Smalley, Chem. Phys. Lett. **138**, 119 (1987).
[23] R. Schäfer, S. Schlecht, J. Woenckhaus, and J. A. Becker, Phys. Rev. Lett. **76**, 471 (1996).
[24] M. F. Jarrold and V. A. Constant, Phys. Rev. Lett. **67**, 2994 (1991).
[25] M. F. Jarrold and J. E. Bower, J. Chem. Phys. **96**, 9180 (1992).
[26] M. F. Jarrold, Y. Ijiri, and U. Ray, J. Chem. Phys. **94**, 3607 (1991).
[27] J. M. Alford, R. T. Laaksonen, and R. E. Smalley, J. Chem. Phys. **94**, 2618 (1991).
[28] J. R. Chelikowsky and N. Binggeli, *Cluster Assembled Materials*, *Materials Science Forum*, edited by K. Sattler (Trans Tech Publications, Ütlihon-Zürich, 1996), Vol. 232, p. 87.
[29] M. Krack and K. Jug, Chem. Phys. **192**, 127 (1995).
[30] D. Porezag, Th. Frauenheim, Th. Köhler, G. Seifert, and R. Kaschner, Phys. Rev. B **51**, 12 947 (1995).
[31] M. R. Pederson and K. A. Jackson, Phys. Rev. B **41**, 7453 (1990); K. A. Jackson and M. R. Pederson, *ibid.* **42**, 3276 (1990); M. R. Pederson and K. A. Jackson, *ibid.* **43**, 7312 (1991).
[32] J. C. Grossman and L. Mitas, Phys. Rev. Lett. **74**, 1323 (1995).
[33] M. V. Ramakrishna and A. Bahel, J. Chem. Phys. **104**, 9833 (1996).
[34] J. Harris, Phys. Rev. B **31**, 1770 (1985).
[35] G. Seifert, H. Eschrig, and W. Bieger, Z. Phys. Chem. (Leipzig) **267**, 529 (1986).
[36] I. Lee, K. J. Chang, and Y. H. Lee, J. Phys.: Condens. Matter **6**, 741 (1994).
[37] C. M. Rohlfing and K. Raghavachari, Chem. Phys. Lett. **167**, 559 (1990).
[38] U. Röthlisberger, W. Andreoni, and P. Giannozzi, J. Chem. Phys. **92**, 1248 (1992).
[39] K. M. Ho, B. C. Pan, C. Z. Wang, J. G. Wacker, D. E. Turner, and D. M. Deaven, Phys. Rev. Lett. (to be published).
[40] D. Porezag and M. R. Pederson, Phys. Rev. B **54**, 7830 (1996).
[41] A. A. Quong, M. R. Pederson, and J. L. Feldman, Solid State Commun. **87**, 535 (1993).
[42] I. Vasiliev, S. Öğüt, and J. R. Chelikowsky, Phys. Rev. Lett. **78**, 4805 (1997).